1963

Electron diffraction investigation of diborane and boron-alkyls

Benjamin Lester Carroll
Iowa State University

ELECTRON DIFFRACTION INVESTIGATION OF DIBORANE AND BORON-ALKYLS

by

Benjamin Lester Carroll

A Dissertation Submitted to the
Graduate Faculty in Partial Fulfillment of
The Requirements for the Degree of
DOCTOR OF PHILOSOPHY

Major Subject: Physical Chemistry

Approved:

Signature was redacted for privacy.

In Charge of Major Work

Signature was redacted for privacy.

Head of Major Department

Signature was redacted for privacy.

Dean of Graduate College

Iowa State University
Of Science and Technology
Ames, Iowa

1963

TABLE OF CONTENTS

		Page
I.	INTRODUCTION	1
	A. Purpose	1
	B. Review of Compounds	2
II.	STRUCTURAL ANALYSIS	5
	A. General Remarks	5
	1. Apparatus	5
	2. Analysis of the radial distribution function	10
	3. Analysis of the intensity function	16
	4. The method of least squares and treatment of errors	19
	B. Structure of Chlorine	22
	C. Structure of Trimethylborine	25
	D. Structure of Diborane and Deuterated Diborane	34
	E. Structure of Tetramethyldiborane	48
	F. Comparison of Structures	58
III.	SUMMARY	63
IV.	LITERATURE CITED	65
V.	ACKNOWLEDGMENTS	69

I. INTRODUCTION

A. Purpose

The purpose of this research was to study how changes in the substituents in certain gaseous molecules affect intramolecular distances, angles between bonds and amplitudes of vibration in these molecules. The compounds selected for this study included diborane, deuterated diborane, trimethylborine, tetramethyldiborane, and chlorine. In order to study the above changes, structural parameters characterizing these molecules had to be determined to a greater degree of accuracy than was known at the time the investigation began. Electron diffraction techniques (1, 2) were used in this investigation for determining structural parameters.

Diborane and deuterated diborane were studied in an effort to ascertain whether an appreciable secondary isotope effect existed in the BB distances.

Trimethylborine and tetramethyldiborane were studied to see what changes take place in the BC distances and angles as the number of atoms bonded to the borons is changed from three to four. It was also of interest to see how the replacement of the terminal hydrogens in diborane with four methyl groups affected the BB distances. It was hoped that something could also be inferred about the internal rotation of the methyl groups in trimethylborine and in tetramethyldiborane.

At the time this investigation originated, a new method was being examined for measuring intensities of electron diffraction patterns. In order to test this method, chlorine, which had been studied previously by Robert DeNeui (3), was reinvestigated.

Conventional procedures used in examining electron diffraction data require the subjective judgement of the person performing the analysis. In order to obtain more objective results and at the same time to eliminate some of the manual computational errors, a method was devised for automating the processes involved in the analysis. Results obtained thus far have been very encouraging.

B. Review of Compounds

The correct molecular geometry of diborane was first proposed by Dilthey (4) in 1921 and later by Core (5) and Nekrason (6). An experimental investigation of the structure was not attempted until Bauer (7) in 1937 used the "visual" electron diffraction method for this purpose. He concluded from his experiments that the configuration was similar to that of ethane. His findings seemed to be consistent with data obtained from mass spectroscopy (8) and x-ray diffraction studies (9).

During the period from 1940 to 1947 various experimental and theoretical studies were made which cast doubt on the ethane type structure (10 - 14). In 1947 and 1948 Price

(15, 16) made a study of the infrared absorption spectrum of diborane in relation to that of ethylene. He found that the absorption spectra were remarkably similar and concluded that diborane had a "bridged hydrogen" structure as postulated by Dilthey. About the same time that Price was making his study, Hedberg and Schomaker (17) reinvestigated diborane using the electron diffraction technique and also concluded that the "bridge" structure was correct.

Discussions of possible electronic configurations of diborane and other boron hydrides have been given by Lipscomb (18, 19), Pitzer (13) and Pauling (20). In 1947 Rundle (21, 22) presented a general theory which could explain the bonding in electron deficient compounds.

The structure of trimethylborine was studied by Levy and Brockway (23) in 1937. Bauer et al. (24 - 26) have done work on various other compounds containing the boron carbon bond.

The approximate structure of tetramethyldiborane was obtained by Hedberg, Jones and Schomaker and cited by Sutton (27).

The interatomic distance in the chlorine molecule was obtained by Pauling and Brockway (28) in 1934 by electron diffraction techniques. Badger as cited by Pauling (28) calculated the interatomic distance in chlorine from the band spectrum reported by Elliott (29) in 1930. The most

recent spectroscopic study was done by Richards and Barrow (30) in 1962.

II. STRUCTURAL ANALYSIS

A. General Remarks

1. Apparatus

All of the experimental intensity data used in this research were taken with the electron diffraction unit (see Figure 1) recently constructed at the Institute for Atomic Research at Iowa State University. The unit is similar to the one at the University of Michigan (1), but was designed to fix the camera distance more precisely and give a greater range in scattering angle. It is equipped with a sector which has an angular opening proportional to the cube of the radius. Three different camera distances are available for use. The two longest distances of 21.4 and 10.7 centimeters were used to obtain the diffraction patterns of the previously mentioned molecules. These two camera distances made it possible to record the scattered intensity from $s = 3.5$ Å^{-1} to $s = 40.0$ Å^{-1} where s is the scattering variable given by $(4\pi/\lambda)\sin(\phi/2)$, λ is the wavelength of the electron beam and ϕ is the scattering angle. The high speed diffusion pumps on the unit, the stability of the beam and the use of appropriate apertures make it possible to obtain clean diffraction patterns beyond $s = 60$ Å^{-1} when the shortest camera distance of 6.8 centimeters is used. The diffraction patterns were recorded on four by five inch

Figure 1. A front and side view of the electron diffraction unit at Iowa State University.

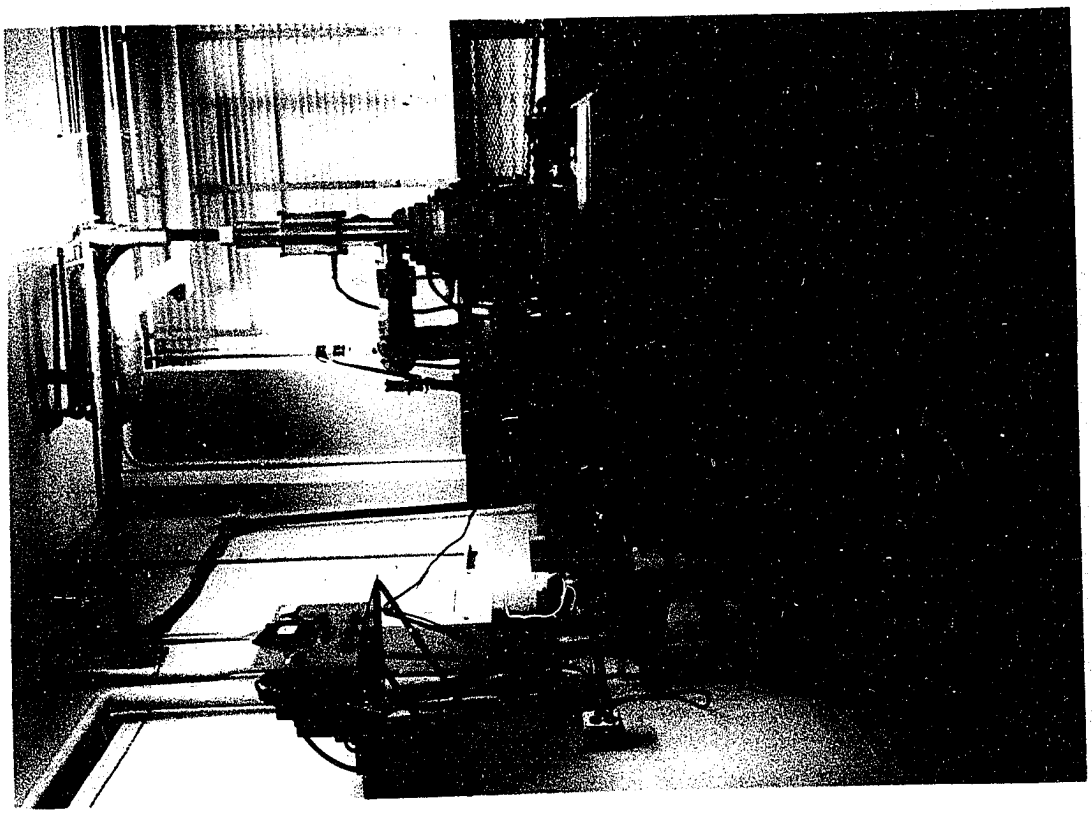

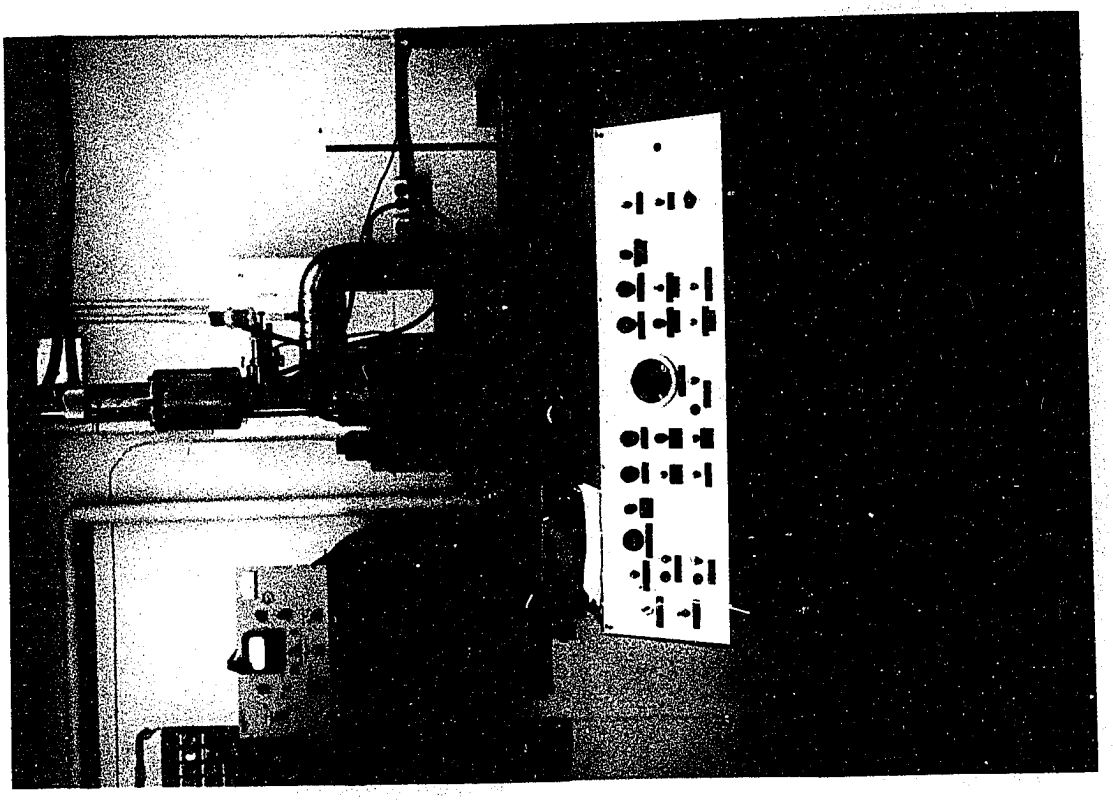

Kodak process plates.

The electron beam was accelerated through a potential of 40,000 volts. The beam current used for diffraction was 0.5 microamperes. This represented about one percent of the total space current emitted by the filament.

The intensities of the diffraction patterns were obtained by scanning completely across the photographic plates from right to left with a microphotometer while the plates were spinning. The spinning helps to average out grain effects, flaws in the emulsion and fluctuations in the pattern caused by small deviations in the beam current (31).

When an electron beam is passed through a stream of gaseous molecules it is diffracted. The diffraction pattern obtained is a series of concentric diffuse rings. The fact that these rings all have a common center makes it possible to find the exact center of the rings in the following way. First an approximate center is found. The plate is then rotated about this center at 5.5 revolutions per second. Next intensity measurements are made beginning at an outer edge of the spinning plate and scanning the plate across the center and out to the opposite edge. Thus two sets of intensity values are obtained for each plate. The correct intensity for a given distance from the true center is the average of two intensities measured at points equidistant from the approximate center. The difference between the two

sets of intensities gives an indication as to the amount of random scatter in the readings caused by fluctuations in the microphotometer and also an estimation of how far off center the plates were when read.

Previous to this research, a microphotometer had been used in conjunction with a recording potentiometer to measure the intensities and positions of the rings in the diffraction patterns. The graphs obtained from the recorder were smoothed and then measured at quarter millimeter intervals. This smoothing process necessarily caused the data points to be correlated to a certain degree. In the work described in this thesis a voltage-to-frequency converter and a direct reading digital voltmeter were used in place of a recording potentiometer. The instrument had a random fluctuation of approximately one-tenth of one percent of the intensity measurements. The measurements were uncorrelated and could be used in determining the experimental error.

The voltage data obtained by this method were converted into intensity values by I.B.M. 650 and 7074 digital computers. The 650 programs were the same as those described by Bonham and Bartell (32). The 7074 programs were similar to those used on the 650, but were rewritten in the fortran programming system. This system allowed the expressions used to be evaluated more rigorously.

2. Analysis of the radial distribution function

Three or four apparently flawless diffraction patterns were chosen from each camera distance and scanned using the microphotometer in conjunction with the voltage-to-frequency converter. The measured voltages were corrected for the drift which was inherent in the instrument and then converted into optical densities and averaged. In the following equations the subscript R will represent measurements which were made while the microphotometer was traveling from the outside of the diffraction pattern towards the inside and L will represent measurements which were made while the microphotometer was traveling from the inside of the diffraction pattern towards the outside. The equation used to compute the effective mean optical densities for structure analysis was

$$1.\quad \overline{D} = (D_R + D_L)/2 - (1/4.6)\left[(\Delta V - \Delta V_0)/(V_M - V_0^f) + \Delta V_0/(V_R - V_0^i)\right]$$

where D_R is $\mathrm{Log}((V_{100}^i - V_0^i)/(V_R - V_0^i))$,

D_L is $\mathrm{Log}((V_{100}^i - V_0^i)/(V_1 - V_0^i))$,

V_0^i is the initial voltage with the shutter closed,

V_{100}^i is the initial voltage at a clear portion of the plate,

V_0^f is the final voltage with the shutter closed,

ΔV_0 is $(V_0^i - V_0^f)$,

ΔV is $(V_R - V_L)$ at $r = 43.75$ millimeters and

V_M is V_R at r = 43.75 millimeters.

The difference between the optical densities from R and L was assumed to be

$$2.\quad \Delta D = (D_R - D_L) + (1/2.3)\left[(\Delta V - \Delta V_0)/(V_M - V_0^f) + \Delta V_0/(V_R - V_0)\right]\left[(r - r_{min})/(r_{max} - r_{min})\right]$$

where r is the plate radius at each observed optical density. The latter portion of Equations 1 and 2 is a correction for the drift in the microphotometer.

A set of optical densities was considered usable if the scatter in ΔD due to centering was no more than three tenths of a percent of the optical densities and that due to random scatter was no more than one tenth of a percent of the optical densities.

The optical densities were converted into average intensities by the equation $\bar{I} = \sum_i^N D_i(1 + \alpha D_i)/N$ where α is a photographic emulsion calibration constant equal to 0.05 (33) and N is the number of plates included in the average. These intensities were leveled by dividing through by theoretical atomic intensities, I_A, where

$$3.\quad I_A = r^3 \sum_k \left[(Z_k - F_k(q))^2 + S_k(q)\right]/q^4$$

and Z is the atomic number of the k^{th} atom,

F(q) is the coherent atomic scattering factor,

S(q) is the incoherent atomic scattering factor,

r is the plate radius corresponding to q and

q is the scattering variable equal to $4\pi(\sin\theta/2)/\lambda$.

The coherent scattering factors were computed from approximations of the type (34, 35)

$$4.\quad F(q) = \sum_n a_n/(1 + bq^2)^{ln}$$

where a, b, and l are constants. The analytical expression used for the inelastic atomic scattering factor (36) was

$$5.\quad S(q) = A_k [\, 1 - 0.200/(1 + 4.252W^2) - 0.302/(1 + 9.907W^2)^2 - 0.217/(1 + 31.9W^2)^4 - 0.216/(1 + 108.2W^2)^8 \,]$$

where W is $0.176\ q/(10Z_k^{2/3})$ and A_k is a constant.

The equation for the total experimental intensity is

$$6.\quad I_t = (\bar{I} - I_{ext})(1 + (r/L)^2)^{3/2}\ \phi_{sc}/I_A$$

where the quantity $(1 + r/L)^2)^{3/2}$ corrects for the inverse square falloff of the intensity on a flat photographic plate. The symbol I_{ext} represents the extraneous intensity approximated by the function $(ar^2 + \alpha(ar^2)^2)E_{ext}$ where a, α, and E_{ext} are constants and ϕ_{sc} is the correction for flaws in the sector.

The total intensity, I_t, obtained in electron diffraction experiments can be expressed as the quantity $I_b(1 + I_M/I_A)$. In this formula I_A is due to scattering from individual atoms and is called the atomic intensity. The symbol I_M is known

as the molecular intensity. The molecular intensity is caused by coherent interference of the diffracted electron beam as a result of the molecular structure. The background, I_b, is a result of errors in theory, scale factor differences between the experimental and theoretical intensities and possibly varying sensitivities of the photographic emulsion. If the total intensity is divided by I_b and the result added to minus one, a ratio of the molecular intensity to the atomic intensity, I_M/I_A, is obtained. This quantity is called the reduced molecular intensity, M(s). It is a particularly convenient function for overlapping the intensity data from different camera ranges and comparing them with a theoretical intensity function.

A radial distribution function (32) can be calculated from the reduced molecular intensity function by the equation

$$7.\quad f(r) = \sum_{s=1}^{s_m} sM_c(s)e^{-bs^2} \sin sr\,\Delta s$$

where $M_c(s)$ is $M(s) + \Delta M(s)$, b is an artificial damping factor (37), $\Delta M(s)$ is a function defined by Bonham and Bartell (38) and s_m is the maximum value of s used.

A constant coefficient theoretical molecular intensity function, $M_c(s)_{th}$, is used in the small s range where experimental intensity data are unobtainable. The constant coefficient theoretical function is given by

$$8.\quad M_c(s)_{th} = \sum_i \sum_j{}' \left[Z_i Z_j e^{-(l_m^2)_{ij} s^2/2} (\cos \Delta\eta_{ij}) \right.$$

$$\left. (\sin s\,(r_g(1)_{ij} + g(s)_{ij}))/s(r_e)_{ij} \right] / \sum_k (Z_k + Z_k^2)$$

where $l_{m_{ij}}$ is the root mean square amplitude of vibration of the ij^{th} atom pair and is defined in (39), cos $(\Delta\eta_{ij})$ is a phase shift correction introduced because of the failure of the Born approximation (40), $r_g(1)_{ij}$ is the center of gravity of the ij^{th} peak in the f(r) function, $g(s)_{ij}$ is a frequency modulation term caused by the anharmonic vibration of the ij^{th} atom pair and $(r_e)_{ij}$ is the equilibrium distance of the ij^{th} atom pair.

The radial distribution function was corrected for integral termination errors (41) by the addition of the equation

$$9.\quad T = (R/2) \sum_j [C_j/(r_e)_j] \exp(-H_j s_m^2)(I_- - I_+)$$

where I_- is $[2H_j s_m \cos(X_j s_m) - X_j \sin(X_j s_m)]/[(2H_j s_m)^2 + X_j^2]$,

I_+ is $[2H_j s_m \cos(p_j s_m) - p_j \sin(p_j s_m)]/[(2H_j s_m)^2 + p_j^2]$,

s_m is the largest experimental s used,

H_j is $(b + l_j^2/2)$,

X_j is $|r - (r_e)_j|$,

p_j is $(r + (r_e)_j)$,

and R, b and c are constants.

The asymmetry of the peaks in the radial distribution is

partially removed by the addition of the equation

$$10.\quad A = -K \sum_j [c_j a_j l_j/(6(r_e)_j(2b + l_j^2)^{1/2})]$$
$$[l_j(r - (r_e)_j)/(2b + l_j^2)]^3 \exp[-(r - (r_e)_j)^2/(4b + 2l_j^2)]$$

where a, K and b are constants. It is necessary to remove the asymmetry from these peaks in order to obtain as close a fit as possible with a synthetic radial distribution function which is calculated from symmetrical gaussian functions.

The corrected radial distribution function, $f_c(r)$, is then analyzed by minimizing the sum of the squares of the differences between the experimental and the synthetic radial distribution function $f(r)_{syn}$. The synthetic function (32) has the form

$$11.\quad f(r)_{syn} = K \sum_j c_j/[r_j(2b + l_j^2)^{1/2}]$$
$$\exp[-(r - r_j)^2/(4b - 2l_j^2)]$$

where K, c_j and b are constants. The parameters obtained from this analysis are the centers of gravity of the peaks in the $f(r)_c$ function. They were corrected to parameters corresponding to the centers of gravity of the peaks in the probability distribution function by the equation (39)

$$12.\quad r_g(0) \simeq r_g(c) + l_a^2/r_e + (3a^2/2r_e - 5a/2r_e^2 + 2/r_e^3$$
$$+ a/(4b + 2l_a^2))l_a^4 + (\text{gas delocalization corrections})$$

where b is the artificial damping factor in $\exp(-bs^2)$,

a is the Morse asymmetry constant,

l_a is the harmonic root mean square amplitude of vibration (39) and

the gas delocalization correction[1] is given in (42).

3. Analysis of the intensity function

The first intramolecular distances obtained from electron diffraction experiments were performed by the "visual" method (28, 43) of analysis. This method consisted of comparing the positions of the apparent maxima and minima and their relative intensities on photographic plates with a series of theoretical intensity curves. The model in best agreement with the experiment was considered to represent the most probable structure of the molecule. This method had the advantage of requiring comparatively little time for an analysis, but was highly subjective and of rather limited accuracy unless the work was done by exceptionally skilled personnel. It also was incapable of yielding all of the parameters obtained by modern methods and techniques.

After the introduction of the rotating sector in 1937, precision recording microphotometers could be used to measure the experimental intensities. The "sector-microphotometer"

---

[1]It was not necessary to make corrections for gas delocalization in these experiments since the pressure build-up in the diffraction chamber was negligible during the time the plates were being exposed.

method along with an improved theory of electron diffraction has led to an almost completely objective procedure for the determination of molecular structures.

The drawing of the background intensity, I_b, in current schemes of analysis is still a partially subjective procedure. Thus the use of an analytical function in place of a manually drawn I_b would greatly help in making an analysis of electron diffraction data more objective. It would also make it possible to automate almost completely the determination of molecular structures from diffraction data.

Since the background intensity is a reasonably smooth function it was thought that it could be approximated by a polynomial series or by a slight modification of a polynomial series. This type of function has the advantage of being easily adapted to automated processes. With it a theoretical intensity function $I_c(s)$ can be calculated. The form of this function is

13. $$I_c(s) = B(s)(RM(s) + 1)$$

where $B(s)$ is the polynomial series approximating I_b and is given by $\sum_i a_i s^i$,

14. $$M(s) = \sum_i \sum_j{}' (Z - F(s))_i (Z - F(s))_j e^{-s^2(l_m^2)_{ij}/2}$$
$$[\cos(\Delta\eta_{ij}) \sin s[(r_g(1))_{ij} + \phi(s)_{ij}]/s(r_e)_{ij}]$$
$$/\sum_k [(Z - F(s))_k^2 + S(s)_k]$$

and R is the index of resolution defined by $M(s)_{exp}/M(s)_{th}$.

The analysis of the experimental intensities was performed by minimizing the sum of the squares of the differences between the experimental intensities and the theoretical intensities. The minimum was reached by varying the structural parameters and the coefficients of the polynomial background.

It soon became apparent that the polynomial function B(s) of low degree was not capable of fitting the background at small s values, as the background bends very sharply in this region. A polynomial of high degree, on the other hand, cannot be trusted to give a smooth background. It was found that by adding an exponential term to the polynomial a smooth background with the proper bend could be obtained. This function has the form

$$15. \quad B(s) = A\, e^{\beta s} + \sum_{i}^{N} a_i s^i$$

where the constant β is determined from the sharpness of the bend in the background function and A is a parameter to be varied during the analysis.

The polynomial backgrounds obtained by letting a computer calculate the polynomial coefficients were usually very smooth functions. They were essentially the same as those obtained when the criterion was used that no negative regions be allowed in the radial distribution function. The structural

parameters were also in agreement within the limits of the estimated error of those obtained from the f(r). Polynomials of degree five to eight gave essentially the same final results.

4. The method of least squares and treatment of errors

There are many methods of fitting an experimental function, Y_e, with a theoretical function, Y_c. The method used in this research was to minimize the sum of the squares of the differences between the theoretical and the experimental functions with respect to the variables characterizing the function.

Suppose that Y is a nonlinear function of the variables t_i. Then the function can be expressed as a linear function by expanding it in a first order Taylor series about the points of t_i'. Thus if $t_i' = \Delta t_i + t_i$, the first order expansion of the function has the form

$$16. \quad Y(t_i + \Delta t_i) = Y(t_i) + \sum_i^M \partial Y/\partial t_i \,|_{t_i} \Delta t_i + V$$

where M is the number of parameters characterizing Y and V is a residue which approaches zero as t_i approaches t_i'.

The least squares criterion states that the best set of parameters characterizing Y_e is obtained when the sum of the squares of the differences $(Y_e - Y_c)$ is a minimum. For this to be so the derivative of this sum with respect to each parameter must be zero. The sum is given by

$$17.\quad Q = \sum_{i}^{N} V_i^2 \, w_i = \sum_{i}^{N} w_i \, (Y_e - Y_c)_i^2$$

where w_i is a weighting function and N is the number of experimental Y_e. After the sum is minimized with respect to each parameter and equated to zero a set of symmetric equations, called the normal equations, can be obtained and solved for Δt_i. The normal equations are

$$18.\quad \sum_{i}^{M} \Delta t_i \sum_{j}^{N} \left(\partial Y_j / \partial t_i \middle| t_i^0 \right) \left(\partial Y_j / \partial t_k \middle| t_k^0 \right) w_j$$

$$= \sum_{j}^{N} w_j \, (Y_e - Y_c(t_i^0)) \left(\partial Y_j / \partial t_k \middle| t_k^0 \right)$$

where $k = 1, 2, \ldots M$ and t_i^0 are initial guesses.

The solution of the normal equations in linear regression theory is usually unique and yields the absolute minimum of Q. In nonlinear problems an iterative process must be used starting with a guess, t_i^0, that is reasonably close to the final converged results. The solutions Δt_i^0 of the normal equations are added to the initial guesses t_i^0 and a better set of estimators t_i^1 are obtained. The parameters t_i^1 now replace t_i^0 as guesses and the process is repeated again and again until the sequence of t_i^k converges.

It can be shown that Δt_i^k must be within a certain limited range of t_i^k for the Taylor expansion of Y to be meaningful. In this research Δt_i^k is modified by the function $\Delta t_{max} \, \Delta t_i^k / |\Delta t_i^k| + \Delta t_{max}$ where Δt_{max} is the maximum value

that Δt_i^k is allowed to assume. Thus when Δt_i^k is small compared to Δt_{max} the function approaches Δt_i^k. When Δt_i^k is large the function approaches Δt_{max}. The value of Δt_{max} that was used in the analysis of the intensity data was 0.1 1a for the amplitudes of vibration and 0.03 for the intramolecular distances.

An estimation of the errors in the structural parameters obtained from the intensity data may be made by using the method derived by Linnik (44) and by Whittaker (45). In this method the assumption is made that the data points are uncorrelated; thus this method of error analysis is applicable to unsmoothed intensity data but not to a radial distribution function unless the correlation between the so-called experimental radial distribution data points is removed by a weighting function.

The errors[2] in the parameters found by analyzing the intensity data are expressed as $\sigma(t_i) = \sqrt{C_{ii}}\ \sigma(I)$ where C_{ii} are the diagonal terms in the inverse normal matrix and $\sigma(I)$ is the standard deviation of the experimental intensity function from the theoretical function.

When a single parameter, t, is varied the expression for the standard error in t takes the form

$$19.\quad \sigma(t) = \left[\sum_i^N (w_i(Y_e - Y_c)^2)/(N-1)\left(\sum_i^N w_i\, \partial Y_i/\partial t\Big|_{t^0}\right)^2\right]^{1/2}$$

[2]For the radial distribution function the errors were determined by the method described by Bonham and Bartell (32).

The standard deviations given by the above equations are a measure of how well the theoretical function fits the experimental data and do not contain the systematic errors due to experimental procedures. The systematic errors must be considered separately. A representative set of experimental errors obtained when careful work is done was tabulated by Kuchitsu and Bartell (39).

B. Structure of Chlorine

The internuclear distance in chlorine and root mean square amplitude of vibration were redetermined in order to evaluate whether a direct reading digital voltmeter could replace the recording potentiometer as the measuring device for the microphotometer. The direct reading microphotometer operates in the following way. A beam of light, after passing through a photographic plate, registers a voltage by means of a photocell. This voltage is continuously converted into a high frequency signal, the frequency of which is proportional to the voltage. The signal is "counted" by a digital scaler which then produces a digital image of the voltage. A determination of the internuclear distance and amplitude of vibration for chlorine had been made previously by DeNeui (3). The original diffraction plates used by DeNeui were precisely the same plates used in the present investigation. DeNeui, however, used a recording potentiometer to measure the voltage appearing at the photocell.

Figure 2. A plot of the experimental radial distribution function for chlorine. The bottom curve is a plot of the difference between the experimental and calculated radial distribution functions.

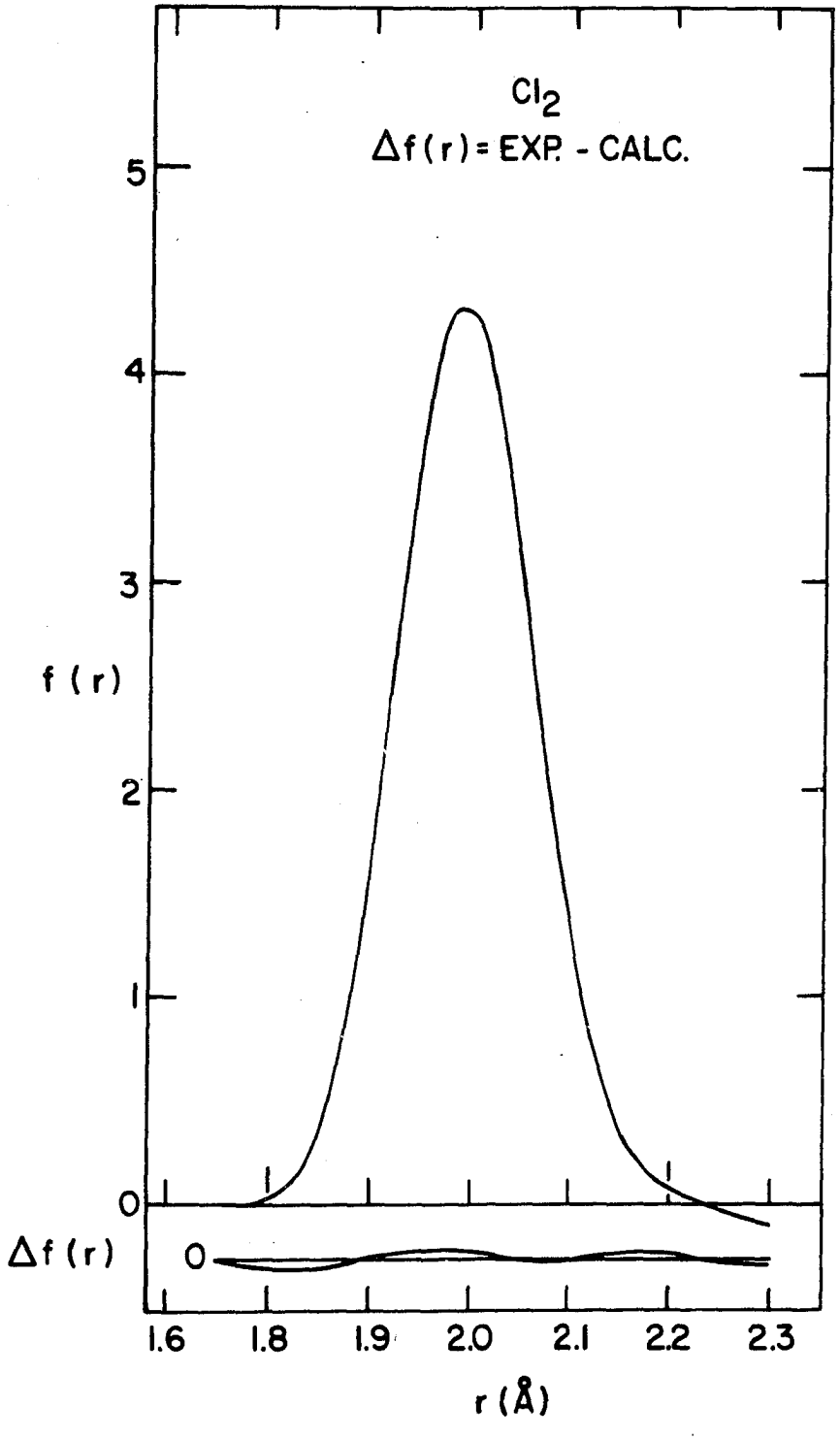
Cl_2
Δf(r) = EXP. - CALC.
5
4
3
f(r)
2
1
0
Δf(r)
0
1.6
1.8
1.9
2.0
2.1
2.2
2.3
r (Å)

The random scatter in the intensity values was approximately 0.1 percent for both methods. The resulting structural parameters were also the same.

The internuclear distance which DeNeui reported contained a small error of computation. When this error is corrected it is found that DeNeui's analysis agrees with the present analysis to within about one part per 10,000 in internuclear distance.

The mean interatomic distance, $r_g(0)$, in chlorine was found to be 1.9927 $\pm$ 0.0045 Å. The amplitude of vibration, $l\alpha$, was found to be 0.0439 $\pm$ 0.0021 Å. The mean distance can be reduced to an equilibrium parameter if a potential function characterizing the molecule is assumed. When a Morse potential is used the value for r_e can be obtained from

$$20. \quad r_e = r_g(0) - (3al\alpha^2/2 + 13a^3l\alpha^4/12 + \ldots) + \delta_{rot}$$

where a is the Morse asymmetry constant and δ_{rot} is a correction for the centrifugal stretching (46) of the bond. The correction, δ_{rot}, is approximately $-kT/r_eK_e$ where k is the Boltzman constant and K_e is the force constant of the bond. When the value of 2.0 $Å^{-1}$ is used for a the corrected equilibrium bond length was 1.9856 $\pm$ 0.0045 Å.

C. Structure of Trimethylborine

A sample of vacuum distilled trimethylborine was obtained from Dr. C. W. Heitsch of Iowa State University.

The sample was stored at -196°C until a short time before its use. The gas entered the diffraction chamber at room temperature and at a pressure of 35 millimeters of mercury. The exposure time was approximately six seconds for the long camera range and approximately thirty seconds for the middle camera range.

After careful examination of all the diffraction patterns taken, three plates from the long camera range and four plates from the middle camera range were selected for microphotometering. The experimental data were converted into total intensities by the use of an I.B.M. 650 digital computer. All other calculations were made on an I.B.M. 7074 digital computer.

The mean distance parameters in molecules, as determined by electron diffraction techniques, are an average over the vibrational motions in the molecules. These vibrations in trimethylborine cause the CC nonbonded distance to appear shorter in comparison with the CB bonds than would be expected if the CBC angle were assumed to be 120°. This effect has been called a "shrinkage" by Bastiansen et al. (47, 48). The experimental "shrinkage" effect in the carbon-carbon distance was approximately 0.0028 Å.

By the use of a computer program obtained from Denis Kohl (49), the carbon-hydrogen nonbonded distances were calculated at ten degree intervals of internal rotation of

the methyl groups about the carbon-boron axis. The number of times that each distance occurs was weighted by the normalized classical probability distribution $P(\theta) = A \exp(-V(\theta)/RT)$. The symbol A is the normalizing factor, $V(\theta)$ is a six-fold potential energy function expressed as $V_0(1 - \cos 6\theta)/2$ and the quantity V_0 is the potential barrier. Synthetic radial distribution functions having different values of V_0 were then calculated. On comparison of the different synthetic curves with the experimental radial distribution function it was found that when V_0 was zero the best fit was obtained.

The free rotation model was to be expected since molecules of nominally the same symmetry have been studied previously by microwave spectroscopy by Naylor and Wilson (50) and by Scott (51) and were found to have low potential barriers. They found that the height of the barrier to internal rotation was 13.77 ± 0.03 calories per mole for methyldifluoroborine and 6.03 ± 0.03 calories per mole for nitromethane. Molecules that have barriers to internal rotation with this small an energy difference appear as free rotators when analyzed by techniques of electron diffraction.

Table 1 shows values for the main parameters obtained from the analysis of the radial distribution function. The structural parameters obtained from an analysis of the radial distribution function, and the least square analysis of the

Figure 3. The solid curves are plots of the experimental total intensity and background functions for the long camera range data of trimethylborine. The experimental background was obtained using the criterion of no negative regions in the radial distribution function. The dashed curves are calculated intensity and background functions obtained by fitting the experimental intensity by the method of least squares.

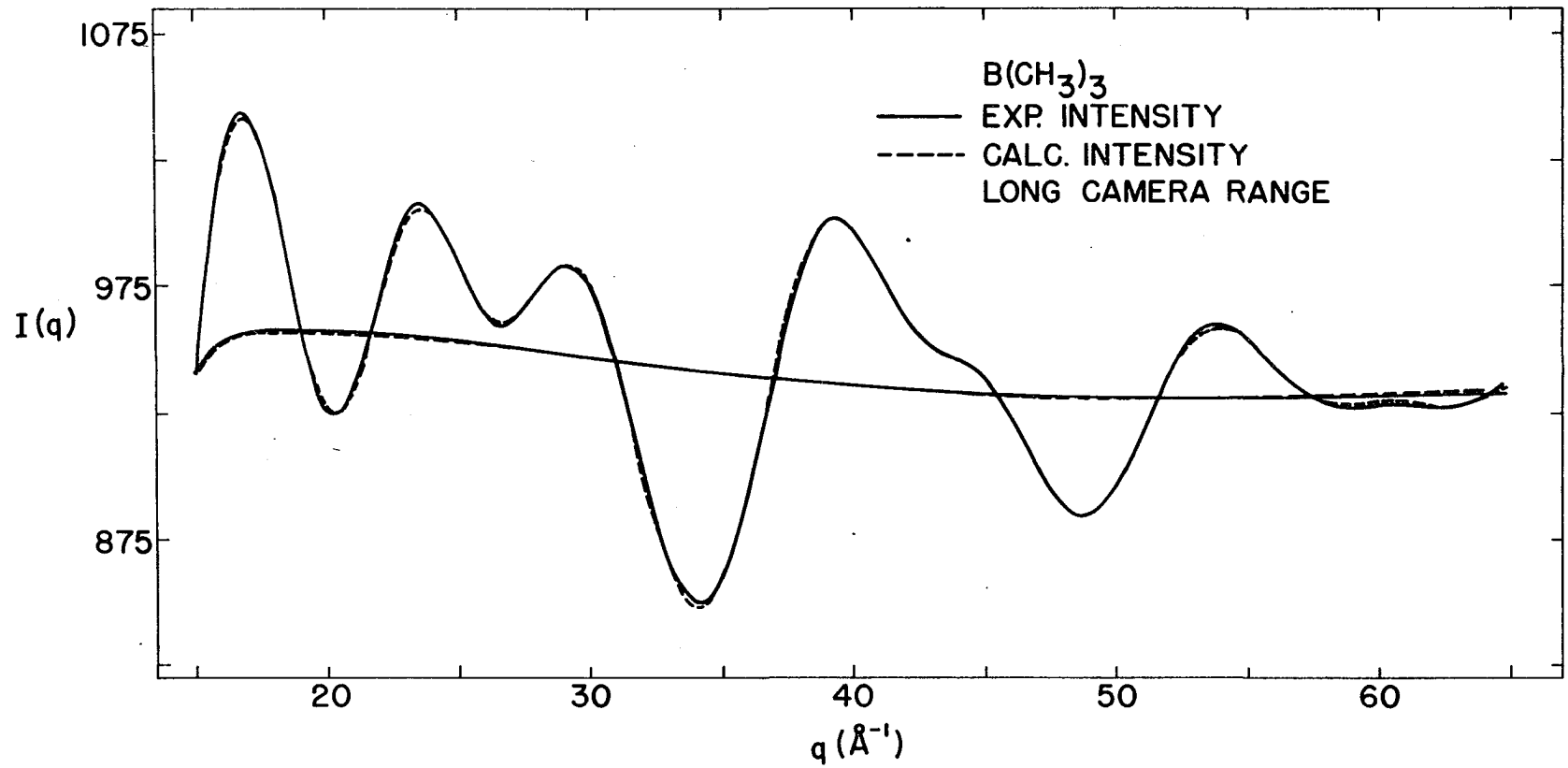
1075
975
875
I(q)
20
30
40
50
60
q (Å⁻¹)
B(CH3)3
EXP. INTENSITY
CALC. INTENSITY
LONG CAMERA RANGE

Figure 4. The solid curves are plots of the experimental total intensity and background functions for the middle camera range data of trimethylborine. The experimental background was obtained using the criterion of no negative regions in the radial distribution function. The dashed curves are calculated intensity and background functions obtained by fitting the experimental intensity by the method of least squares.

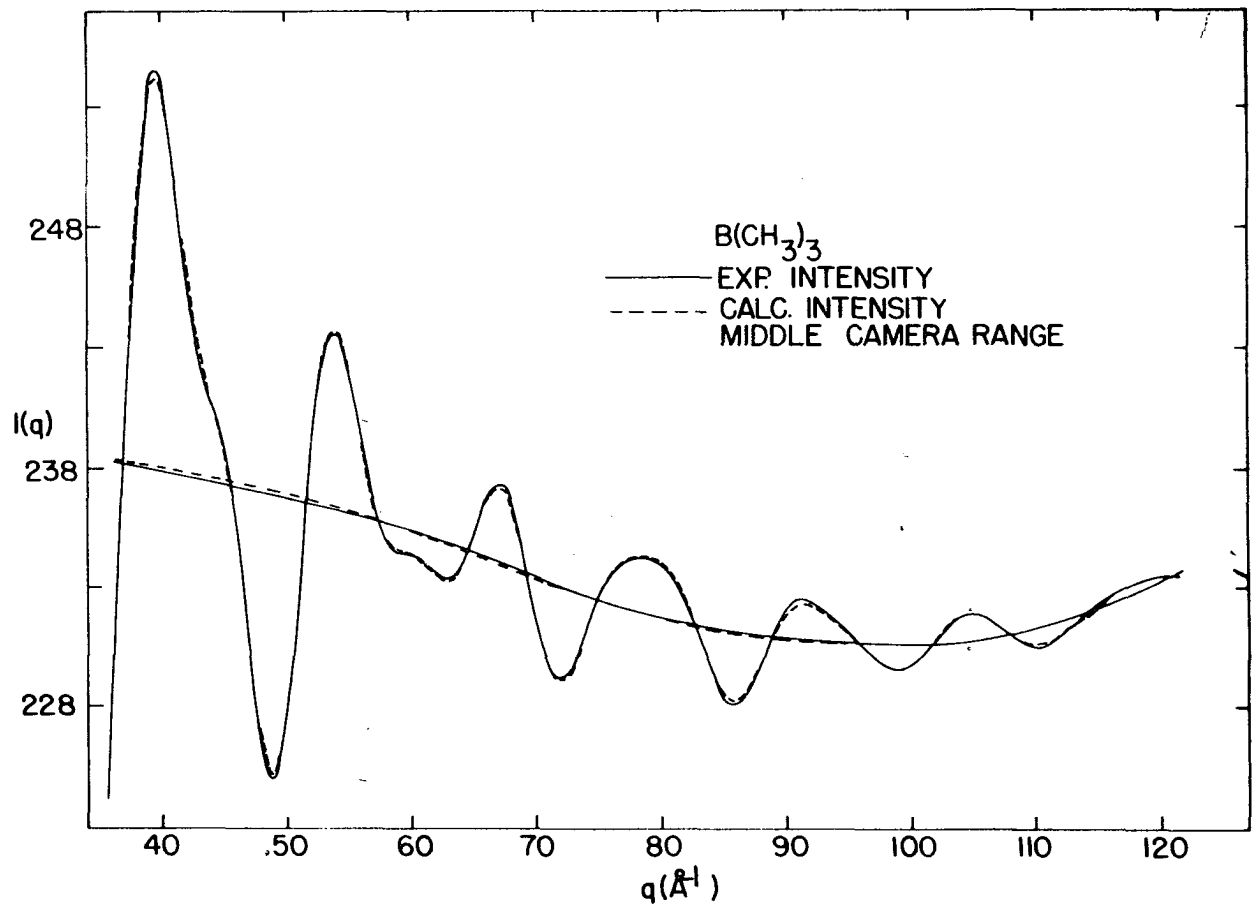
248
238
228
I(q)
B(CH3)3
EXP. INTENSITY
CALC. INTENSITY
MIDDLE CAMERA RANGE
40
.50
60
70
80
90
100
110
120
q(Å-1)

Figure 5. A plot of the experimental radial distribution function of trimethylborine. The lower curve is a plot of the difference between the experimental and calculated radial distribution functions.

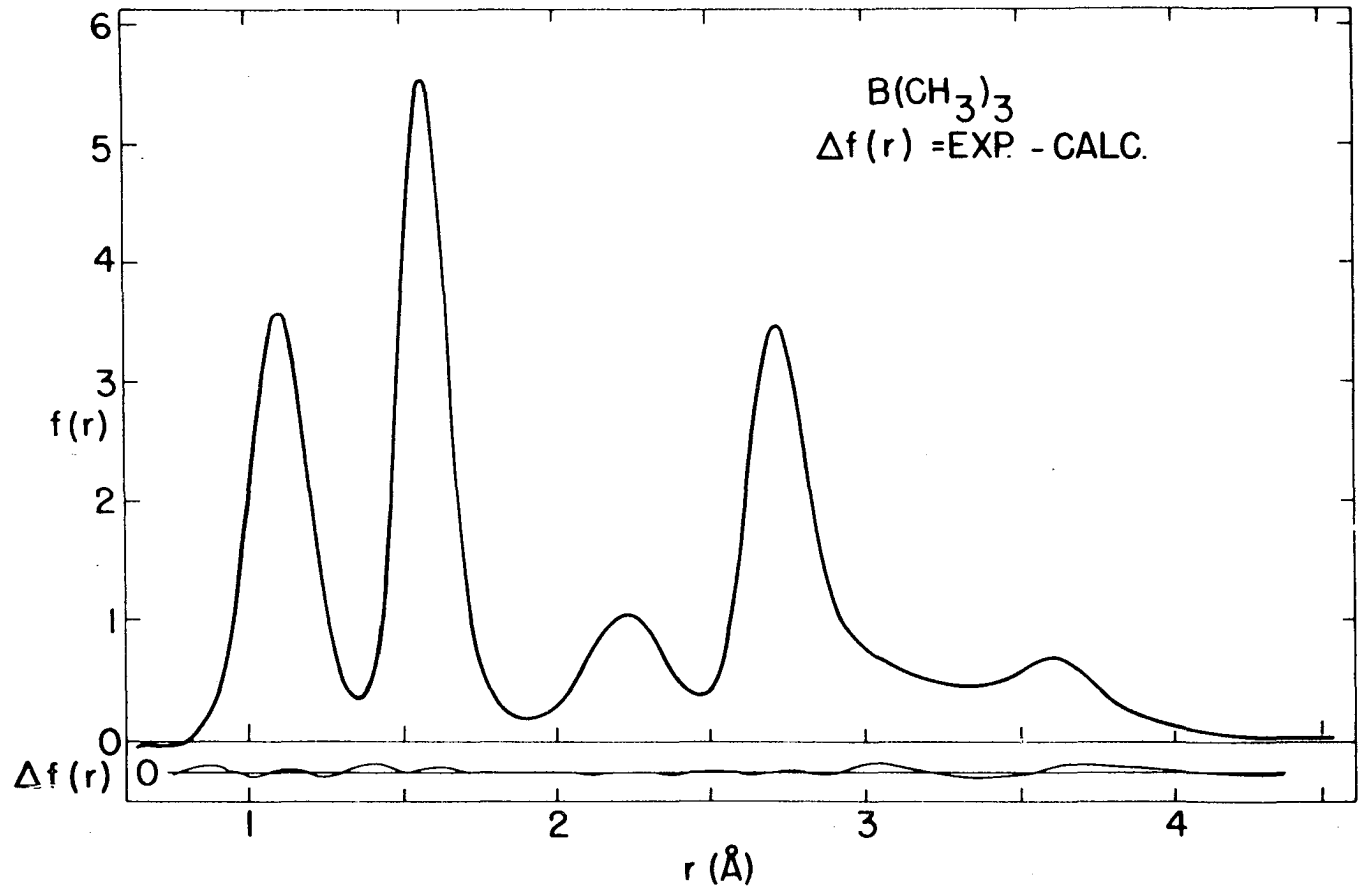
B(CH3)3
Δf(r) =EXP. - CALC.
f(r)
Δf(r)
r (Å)
0
1
2
3
4
5
6

Table 1. Molecular parameters for trimethylborine obtained from the radial distribution function

Distance	$r_g(1)$	$r_g(0)$	$\sigma(r)$	$l\alpha$	$\sigma(l)$
B-C	1.5758	1.5778	0.0011	0.0537	0.0014
C ... C	2.7233	2.7255	0.0013	0.0760	0.0017
B ... H	2.2377	2.2451	0.0051	0.1274	0.0046
C-H	1.1088	1.1150	0.0022	0.0818	0.0024

$\angle$ CBC = 119.5 $\pm$ 0.2°

$\angle$ BCH = 111.8 $\pm$ 0.2°

Index of Resolution 1.00 $\pm$ 0.03

long and middle intensity data were the same to within the range of the estimated errors.

D. Structure of Diborane and Deuterated Diborane

Samples of spectroscopically pure diborane and deuterated diborane were obtained from Dr. C. W. Heitsch of Iowa State University. The samples were stored at -196°C until a short time before they were used. The samples were introduced into the diffraction chamber at room temperature and at a pressure of thirty-five millimeters of mercury. The exposure times were approximately seventeen seconds for the long camera range and approximately ninety seconds for the middle camera range. The pressure in the diffraction chamber was about

5×10^{-5} millimeters of mercury and increased to a maximum of 8×10^{-5} millimeters of mercury as the gas entered the chamber. The I.B.M. 650 digital computer was used exclusively in analyzing the diffraction patterns of these two compounds.

The effect of replacing the hydrogens with deuteriums was very noticeable in the radial distribution functions of the two compounds. The BD peaks and also the DD peaks were sharper than the corresponding peaks in B_2H_6. This was caused by the smaller amplitudes of vibration associated with the heavier deuteriums.

In B_2H_6 the BB distance appeared to be 0.0038 ± 0.0059 Å longer than in B_2D_6. The mean BBH_t angle was found to be 119.9 ± 0.6 degrees and the corresponding angle in B_2D_6 was found to be 118.8 ± 1.6 degrees. The mean H_bBH_b angle was 97.0 ± 0.7 degrees. The corresponding angle in B_2D_6 was the same.

The index of resolution was unity. This and the fact that there was no observed build up of gas pressure in the diffraction chamber as the patterns were recorded lead to a negligible correction to the intramolecular distances due to the scatter of electrons by delocalized gas.

Tables 2 and 3 give the parameters obtained from an analysis of the radial distribution function.

The reason for the relatively high uncertainties in the diborane and deuterated diborane data should be pointed out.

Figure 6. A plot of the experimental total intensity and background function for the long camera range data for diborane.

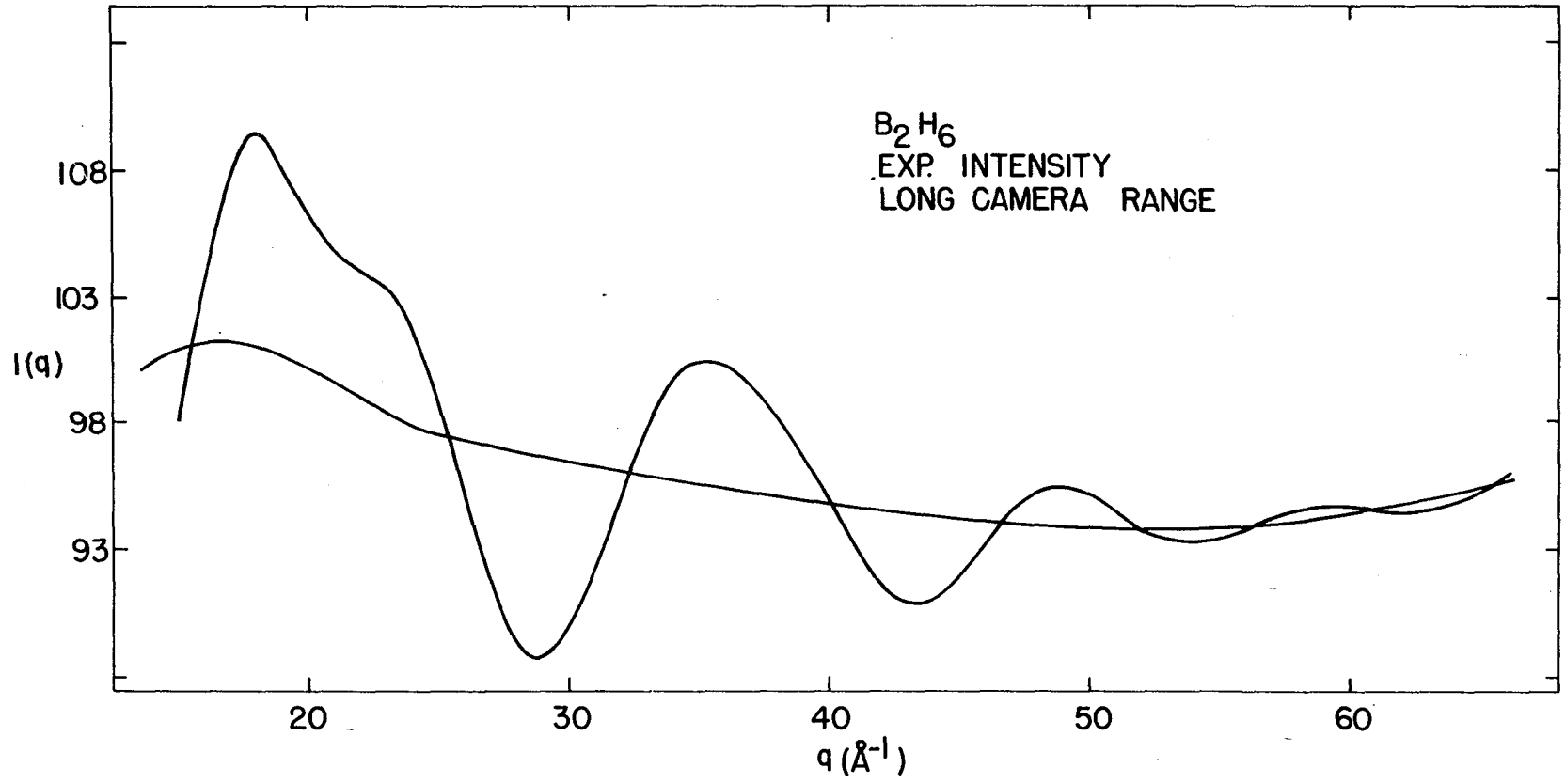
$B_2 H_6$
EXP. INTENSITY
LONG CAMERA RANGE
108
103
98
93
I(q)
20
30
40
50
60
q (Å^{-1})

Figure 7. A plot of the experimental total intensity and background function for the middle camera range data of diborane.

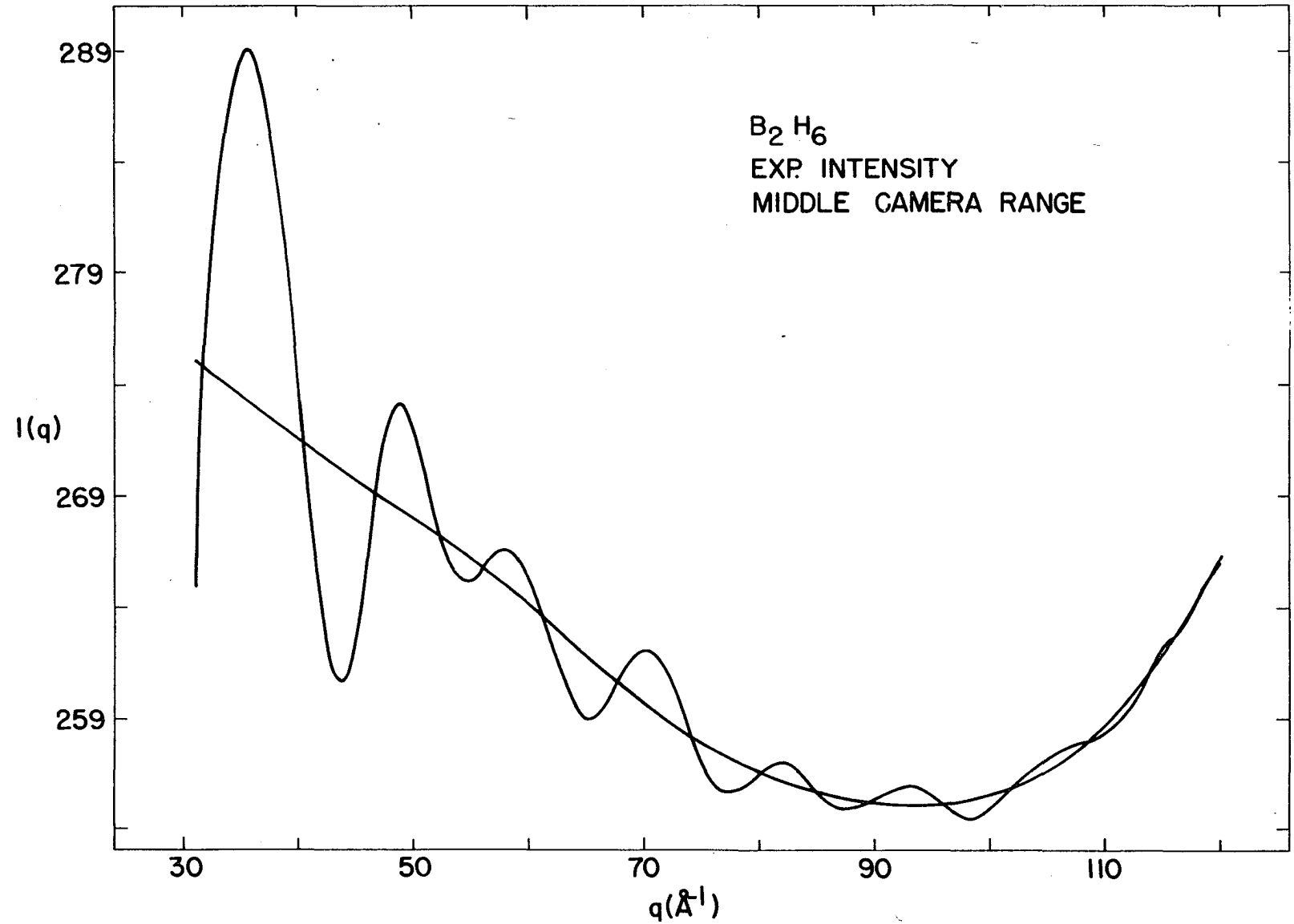
289
279
269
259
I(q)
30
50
70
90
110
q(Å⁻¹)
B2 H6
EXP. INTENSITY
MIDDLE CAMERA RANGE

Figure 8. A plot of the experimental total intensity and background function for the long camera range data of deuterated diborane.

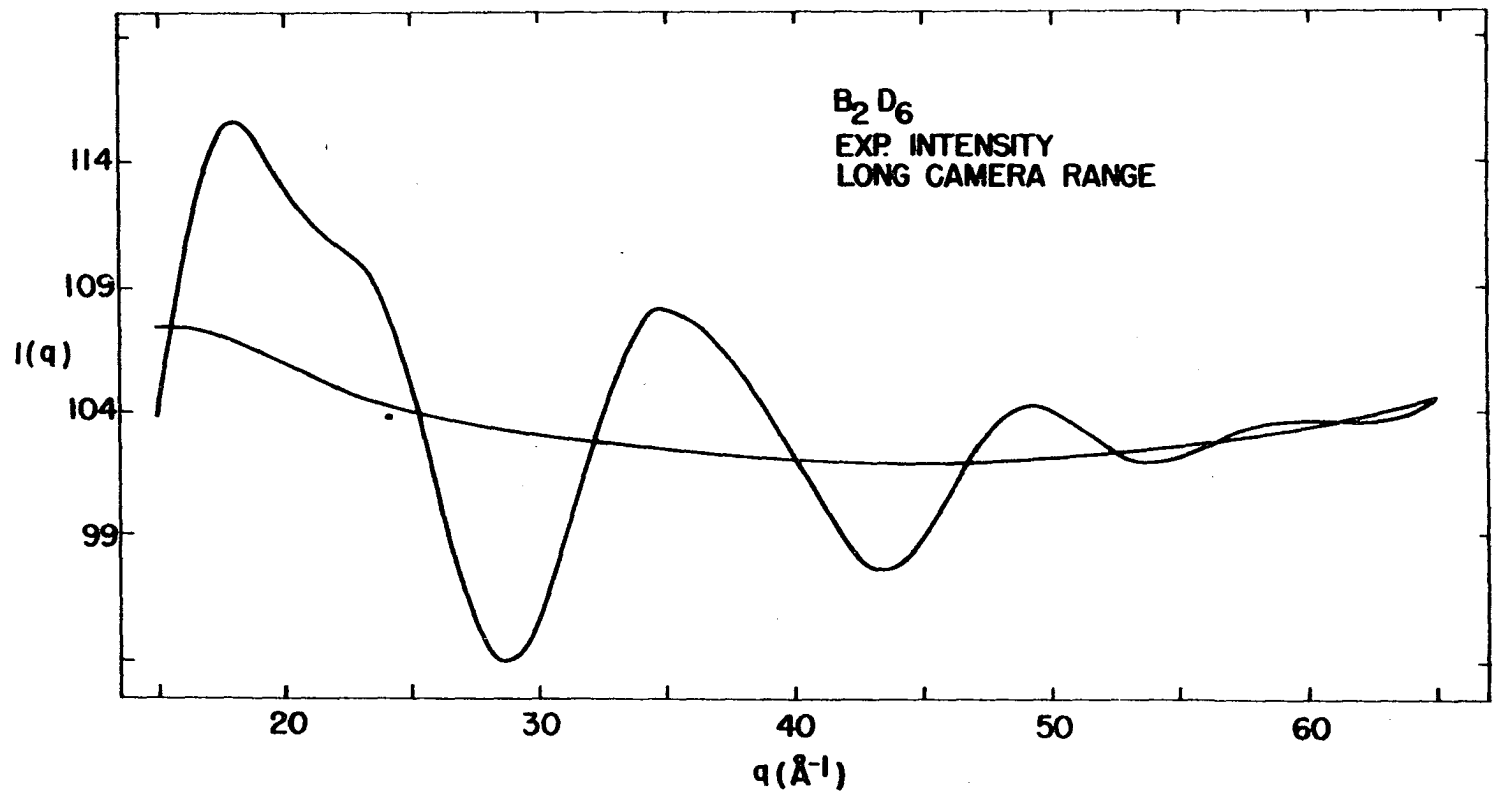
$B_2 D_6$
EXP. INTENSITY
LONG CAMERA RANGE
114
109
104
99
I(q)
20
30
40
50
60
q(Å^{-1})

Figure 9. A plot of the experimental total intensity and background function for the middle camera range data of deuterated diborane.

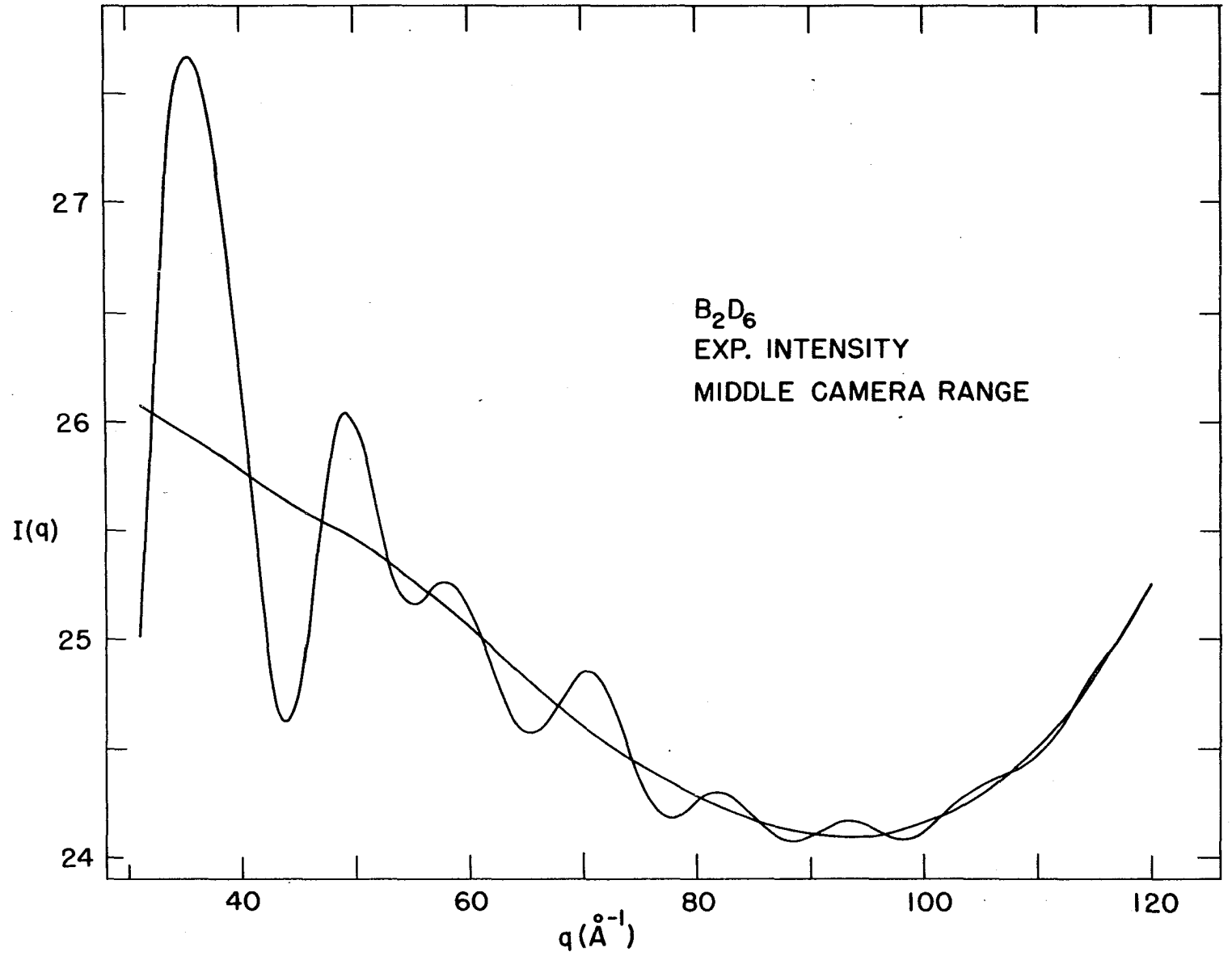
27
26
25
24
I(q)
40
60
80
100
120
q(Å⁻¹)
B2D6
EXP. INTENSITY
MIDDLE CAMERA RANGE

Figure 10. The dashed curve is a plot of the experimental radial distribution function of diborane. The solid curve is a plot of the experimental radial distribution function of deuterated diborane. The lower curves are plots of the differences between the experimental and calculated radial distribution functions.

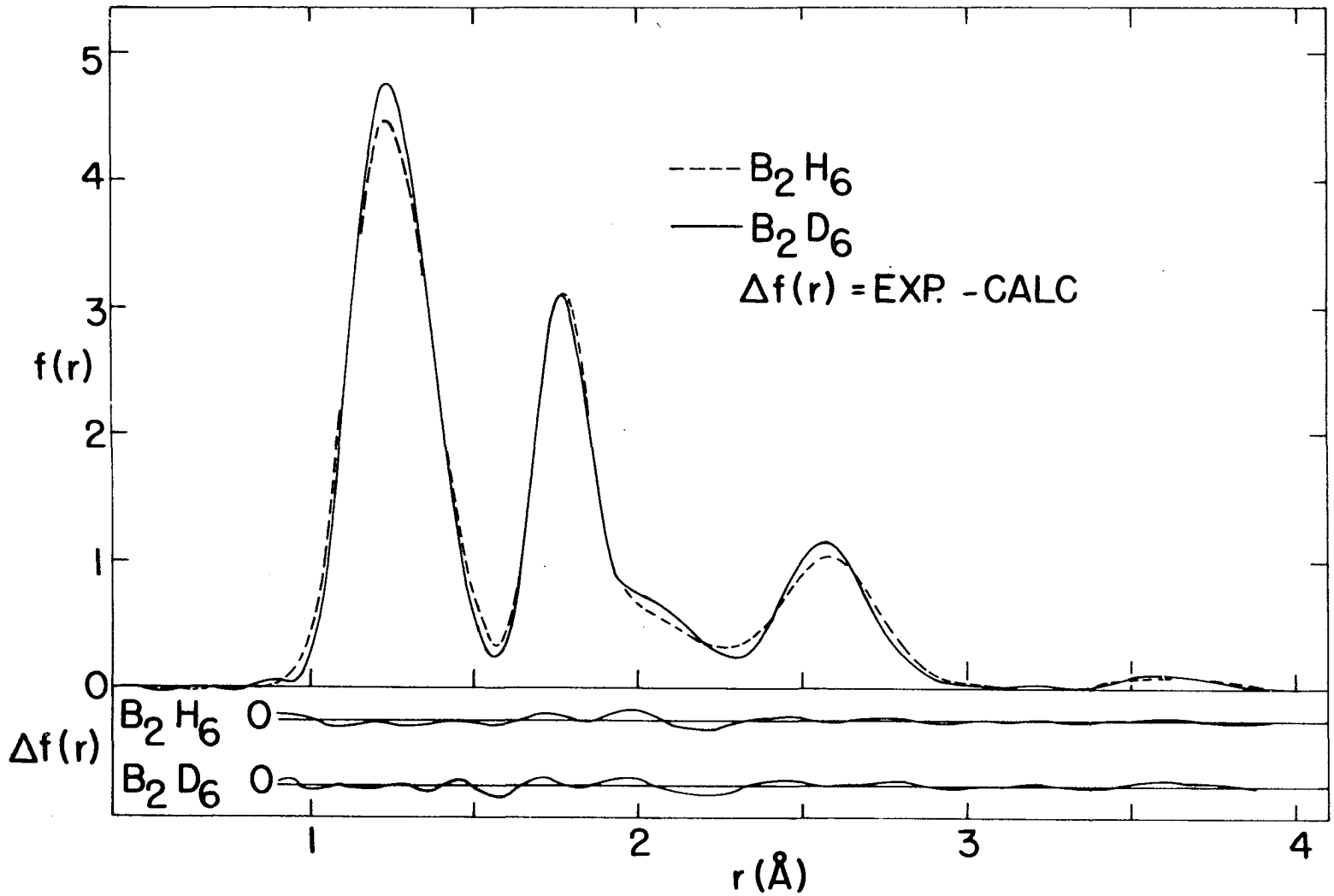
5
4
3
2
1
0
f(r)
B_2H_6
B_2D_6
Δf(r) = EXP. - CALC
Δf(r)
B_2H_6 0
B_2D_6 0
1
2
3
4
r (Å)

Table 2. Structural parameters obtained from the radial distribution function of B_2H_6

Distance	$r_g(0)$	$r_g(1)$	$\sigma(r)$	la	$\sigma(1)$
BB	1.7750	1.7729	0.0040	0.0607	0.0025
BH_t	1.196	1.191	0.016	0.074	0.016
BH_b	1.339	1.334	0.016	0.086	0.016
B...H	2.5881	2.5826	0.0088	0.1181	0.0053
BH_{ave}[a]	1.2670		0.0045		
ΔBH[b]	0.143		0.015		

$\angle BBH_t = 119.9 \pm 1.6°$

$\angle H_bBH_b = 97.0 \pm 0.7°$

Index of Resolution = 1.00 ± 0.03

[a]Center of gravity of boron-hydrogen composite peak.

[b]Split between BH_t and BH_b.

After the B_2H_6 and B_2D_6 plates were taken and analyzed it was discovered that the sector mounting was slipping inside the steel ball bearing race as the sector rotated. This caused the phase angle of the known magnetic disturbance associated with the imperfectly demagnetized race to vary with respect to the sector. When the phase angle of the disturbance is fixed, which it is when the mounting is properly locked, the error can be accurately corrected for.

Table 3. Structural parameters obtained from the radial distribution function of B_2D_6

Distance	$r_g(0)$	$r_g(1)$	$\sigma(r)$	$l\alpha$	$\sigma(l)$
BB	1.7712	1.7692	0.0044	0.0594	0.0024
BD_t	1.198	1.194	0.016	0.065	0.016
BD_b	1.334	1.329	0.016	0.076	0.016
B...D	2.5723	2.5678	0.0082	0.1056	0.0051
BD_{ave}[a]	1.2657		0.0045		
ΔBD[b]	0.136		0.015		

$\angle BBD_t = 118.8 \pm 1.6°$

$\angle D_bBD_b = 96.8 \pm 0.7°$

Index of Resolution = 1.00 ± 0.03

[a]Center of gravity of boron-deuterium composite peak.

[b]Split between BD_t and BD_b.

In the diborane plates, however, the disturbance was of unknown direction, and hence had to be assessed as an additional error. It amounted to approximately 0.2 percent of the interatomic distances.

The particularly large uncertainties in the BH_t and BH_b bonds are a result of the extensive overlap between the two radial distribution peaks. The center of gravity of the composite peak can be determined to 0.0045 Å. The difference

between the two distances, on the other hand, can be determined to only 0.015 Å.

E. Structure of Tetramethyldiborane

A sample of vacuum distilled tetramethyldiborane was obtained from Dr. C. W. Heitsch of Iowa State University. The sample was stored at -196°C until a short time before it was introduced into the diffraction chamber. The sample was pumped on for 20 minutes at -78°C before each set of five diffraction patterns was taken. The sample was allowed to warm up to -11°C before introducing it into the diffraction chamber. The sample had a vapor pressure of approximately 26 millimeters of mercury at -11°C. The plates were exposed for 6 seconds at the long camera range and for 18 seconds at the middle camera range.

In order to determine the skeletal parameters that were obscured by the nonbonded BH and CH intramolecular distances in the radial distribution curve, an analysis by the method of least squares was performed on the middle camera range intensity data. It was shown by using models with different methyl group configurations that the distances with high scattering power and low amplitudes of vibration were mostly independent of the methyl configurations in the middle range data. Using the structural parameters that were determined in the above way, five models were calculated using different potential barriers to restrict the internal rotation of the

Figure 11. A plot of the experimental total intensity and background functions for the long camera range data of tetramethyldiborane.

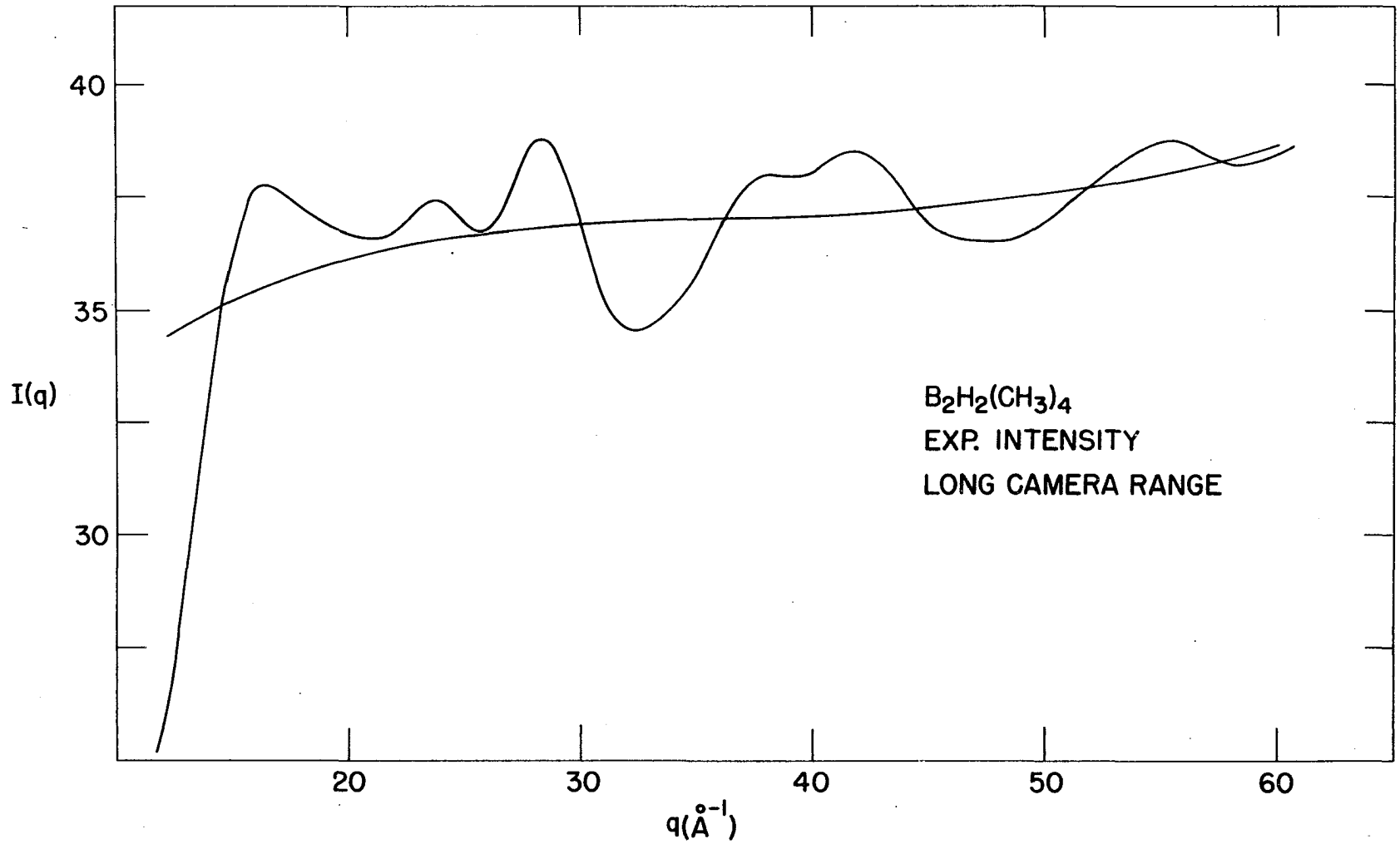
40
35
30
I(q)
20
30
40
50
60
q(Å⁻¹)
B2H2(CH3)4
EXP. INTENSITY
LONG CAMERA RANGE

Figure 12. A plot of the experimental total intensity and background functions for the middle camera range data of tetramethyldiborane.

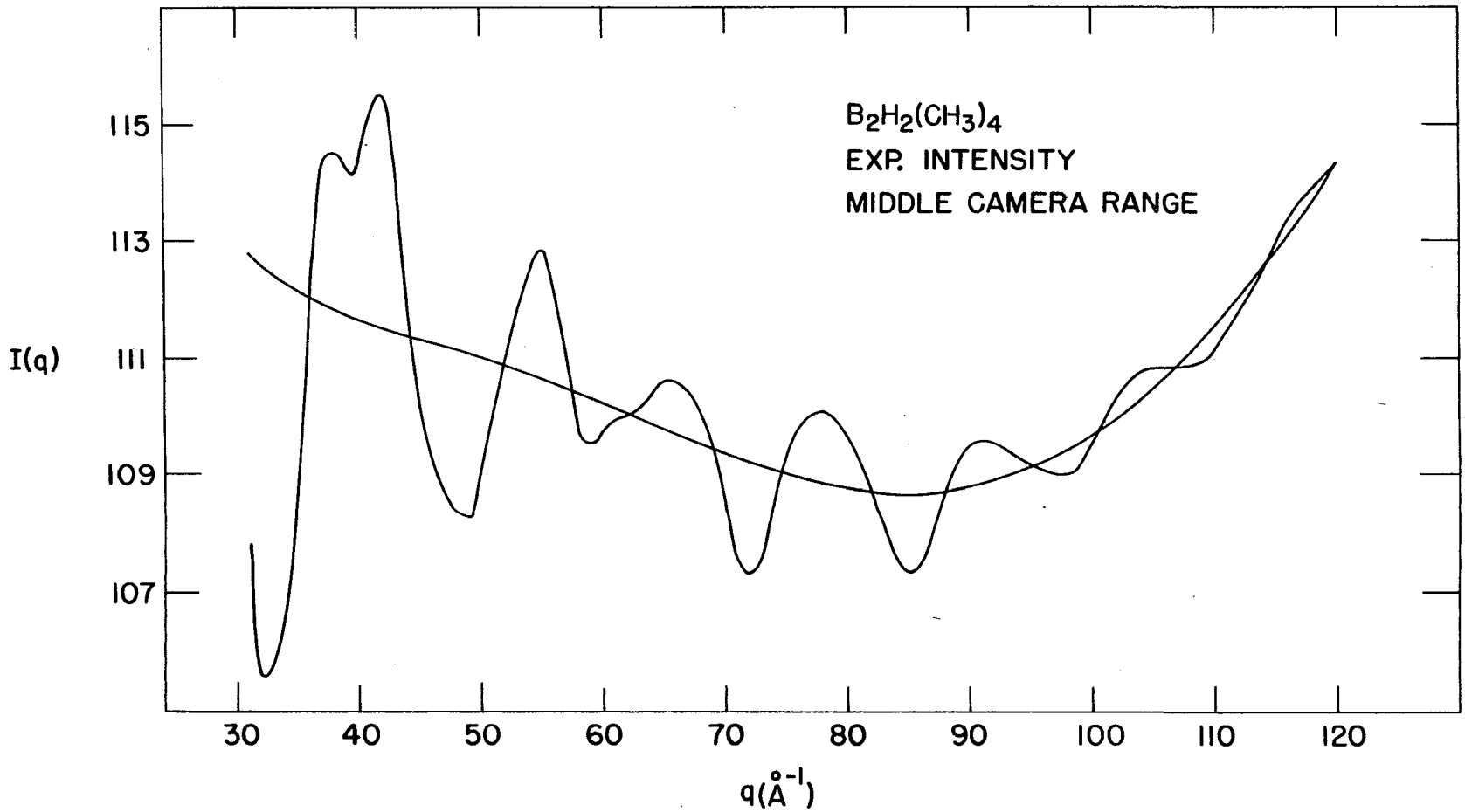
$B_2H_2(CH_3)_4$
EXP. INTENSITY
MIDDLE CAMERA RANGE
I(q)
115
113
111
109
107
30
40
50
60
70
80
90
100
110
120
q(Å^{-1})

Figure 13. The solid curves are experimental radial distribution functions calculated at potential barriers of 0, 1/2, 1 and 2 kcal per mole. The dashed curves are the calculated radial distribution functions corresponding to the same potential barriers.

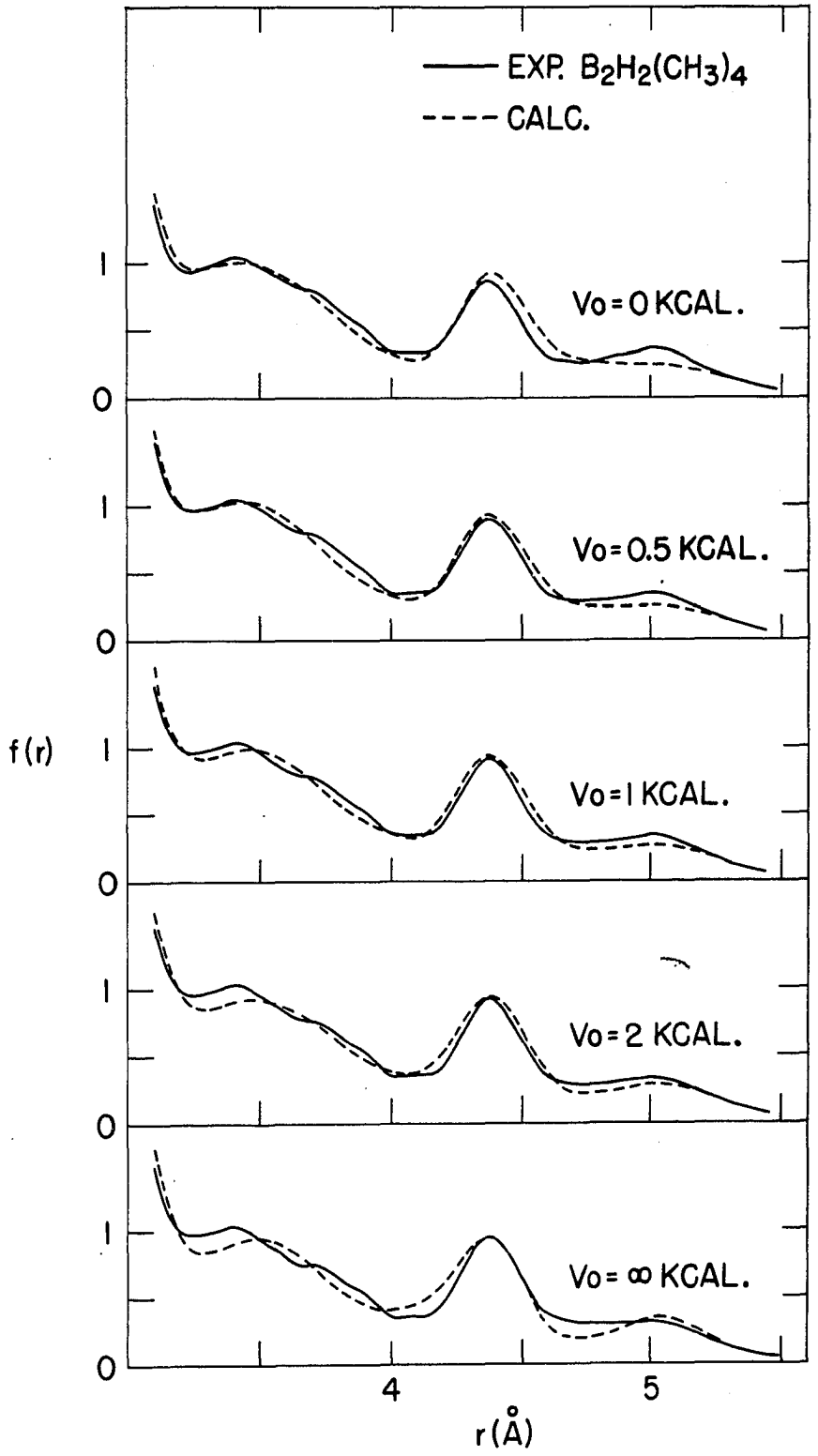
EXP. $B_2H_2(CH_3)_4$
CALC.
Vo = 0 KCAL.
Vo = 0.5 KCAL.
Vo = 1 KCAL.
Vo = 2 KCAL.
Vo = ∞ KCAL.
f(r)
1
0
4
5
r(Å)

Figure 14. A plot of the experimental radial distribution function of tetramethyldiborane. The lower curve is a plot of the difference between the experimental and calculated radial distribution functions.

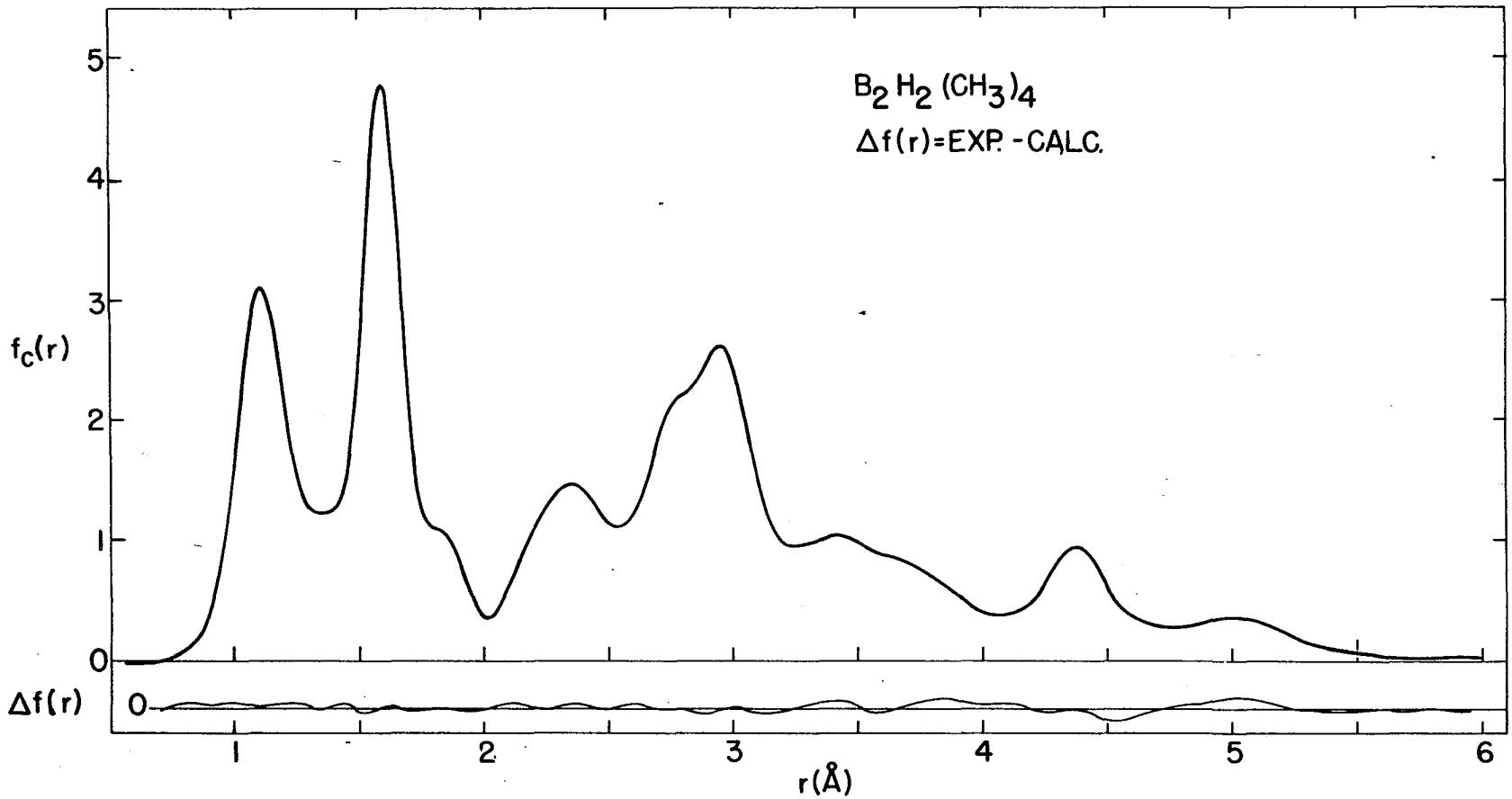
$B_2H_2(CH_3)_4$
Δf(r)=EXP.-CALC.
$f_c(r)$
Δf(r)
r(Å)
0
1
2
3
4
5
6

Table 4. Structural parameters for tetramethyldiborane

Distance	$r_g(0)$	$r_g(1)$	$\sigma(r)$	$l\alpha$	$\sigma(l\alpha)$
B-C	1.5899	1.5878	0.0016	0.0574	0.0016
B...C	2.9588	2.9559	0.0080	0.0929	0.0053
C-H	1.1218	1.1152	0.0032	0.0851	0.0031
B...B	1.8400	1.8376	0.0069	0.0664	0.0044
B-H_b	1.3642	1.3627	0.0063	0.0459	0.0063
B...H	2.2742	2.2687	0.0080	0.1118	0.0056
C...C	2.7327	2.7307	0.0080	0.0738	0.0052

$\angle$ CBC = 120 $\pm$ 1.5°

$\angle$ BCH = 109.2 $\pm$ 0.6°

$\angle H_bBH_b$ = 95.2 $\pm$ 0.5°

Index of Resolution = 1.00 $\pm$ 0.03

methyl groups. The results are shown graphically in Figure 13. A comparison of observed data and calculated curves suggests that the barrier to internal rotation is approximately 700 calories per mole.[3]

An analysis of the radial distribution function gave essentially the same parameters for the CH bond, the CB

[3]It was assumed in the calculation of the models used to determine the potential barrier that the configuration of the tetramethyldiborane skeleton (not counting the hydrogens on the methyl groups) was C_{2v}.

bond, the BH_b bond and the BB distance as the independent analysis of the middle camera range data. Table 4 lists the structural parameters characterizing tetramethyldiborane.

F. Comparison of Structures

A comparison of results obtained from various structural determinations of diborane, tetramethyldiborane, trimethylborine and compounds containing similar bonds is made in Table 5. The results show that the boron-carbon bond is longer in tetramethyldiborane than in trimethylborine by about 0.014 Å. The CBC angle, however, is about the same in both compounds.

The high uncertainties in most of the parameters taken from the literature make it difficult for definitive comparisons to be made. The boron-boron distance does, however, appear to be a function of the substituents attached to the boron atom. For example the boron-boron distance in diborane increases approximately 0.06 Å when some of the hydrogens are replaced by methyl groups. Replacing a hydrogen with a bromine atom, however, appears to have little effect on the distance. When one of the bridging hydrogens is replaced by an amino or dimethylamino group the boron-boron distance is increased by about 0.08 Å. Substitution of the hydrogens with deuteriums gives an indication of a secondary isotope effect. The shift is not significant, though, when viewed in terms of Cruickshank's (52) criterion.

Table 5. Comparison of results of various structural determinations

Molecule	BC	BB	BH_t	BH_b	CH	$\angle H_tBH_t$ degrees	$\angle CBC$ degrees	Reference
B_2H_6		1.770 ±.013	1.187 ±.030	1.334 ±.027		121.5 ± 7.5		(17)
B_2H_6		1.775 ±.004	1.196 ±.016	1.339 ±.013		120.2 ± 1.6		present study
B_2D_6		1.771 ±.004	1.198 ±.016	1.334 ±.016		118.8 ± 1.6		present study
$B(CH_3)_3$	1.56 ±.02						120 ±3.4	(23)
$B(CH_3)_3$	1.578 ±.001				1.115 ±.002		119.5 ±.2	present study
$B_2H_2(CH_3)_4$	1.59 (app.)[a]	1.84 (app.)					120 (app.)	(27)
$B_2H_2(CH_3)_4$	1.590 ±.002	1.840 ±.007		1.364 ±.006	1.122 ±.003		120 ±1.5	present study
$B_2H_3(CH_3)_4$	1.61 (app.)	1.86 (app.)					125 (app.)	(27)

[a]Approximate.

Table 5. (Continued)

Molecule	BC	BB	BH_t	BH_b	CH	$\angle H_tBH_t$ degrees	$\angle CBC$ degrees	Reference
$B_2H_5(NH_2)$		1.93 ±.09	1.15 ±.09	1.35 (app.)				(53)
$B_2H_5N(CH_3)_2$		1.92 ±.11						(53)
B_2H_5Br		1.770 ±.013						(27)
B_4H_{10}		1.75 1.85	1.19	1.33-1.43				(54, 55)
B_5H_9		1.687 ±.005	1.23 ±.07	1.36 ±.08				(54, 56)
		1.800 ±.003						
B_6H_{10}		1.60 ±.01	1.22 ±.06	1.38 ±.08				(57)
		1.74 ±.01						
		1.74 ±.01						
		1.79 ±.01						

Table 5. (Continued)

Molecule	BC	BB	BH_t	BH_b	CH	$\angle H_tBH_t$ degrees	$\angle CBC$ degrees	Reference
$B_{10}H_{14}$		1.73 to 2.01	1.28	1.34 to 1.40				(58, 59)
BH_3CO	1.57 ±.03							
	1.540		1.194			113.9		(24, 60)
$(BH_3CO)_3$	1.57 ±.03							(25)
B_2CL_4		1.80 ±.05						(61)
$BF(CH_3)_2$	1.55 ±.02							(26)
BF_2CH_3	1.60 ±.03							(26)

The HBH angle in diborane is about 120°. The HBH angle in borine carbonyl, in contrast, is about 113.9°.

The best agreement between experimental and calculated data for trimethylborine was obtained when the methyl groups were considered to rotate freely about the boron-carbon bond. This is consistent with the results of microwave work for nitromethane and methyldifloroborine (50). Some information was also gained concerning the configuration of the methyl groups in tetramethyldiborane from a study of the experimental radial distribution function. These results indicated that the methyl groups were in a staggered configuration with a three-fold potential barrier to internal rotation about the boron-carbon bond. The height of the barrier appeared to be approximately 700 calories per mole. This is intermediate between the value for trimethylborine and values encountered in tetrahedral frameworks with electron pair bonds.

The equilibrium bond length in chlorine was found to be 1.986 ± 0.005 Å, including the uncertainty due to the magnetic disturbance. This is in satisfactory agreement with the spectroscopic results of both Badger as cited by Pauling (28) and of Richards and Barrow (30). The spectroscopic results were 1.988 Å and 1.989 Å respectively.

III. SUMMARY

A reinvestigation of diffraction patterns of chlorine confirmed that a direct reading microphotometer could be used with confidence in measurements of electron diffraction intensities. The equilibrium bond length determined by this method was within 0.0001 Å of DeNeui's earlier result obtained from the same patterns by a different technique.

A procedure for the analysis of electron diffraction intensities was devised which almost completely eliminated the manual manipulation of data and the need for subjective judgement formerly made by the operator. An outstanding feature of this procedure is that the molecular structure parameters which characterize the data are determined by an automatic program that fits the experimental intensity with a theoretical function. This is done by an iterative method of least squares. For additional verification of the final results an experimental radial distribution function was also calculated and analyzed.

Compounds selected for structural studies included trimethylborine, diborane, deuterated diborane and tetramethyldiborane. Experimental results are listed in Tables 1 through 4. In Table 5 the principal results are summarized and compared with parameters reported in the literature for related compounds. The C-B bond length in trimethylborine (1.578 Å) was shorter than that in tetramethyldiborane

(1.590 Å). The C-H distance was also shorter in trimethylborine (1.115 Å) than in tetramethyldiborane (1.122 Å). These two molecules have BCH angles which are respectively 111.8° and 109.2°. In the four compounds studied, the CBC and terminal HBH angles were approximately 120°.

A difference of 0.065 ± 0.008 Å was found when the B-B distance in diborane (1.775 Å) was compared with that in tetramethyldiborane (1.840 Å). The bridge HBH angle was 97° for diborane and 95° for tetramethyldiborane.

Internal rotation of the methyl groups about the C-B axis in trimethylborine was found to be unrestricted. In tetramethyldiborane, however, the methyl groups appeared to be in a staggered configuration with a three-fold potential barrier to internal rotation of approximately 700 calories per mole.

IV. LITERATURE CITED

1. Bartell, L. S. and Brockway, L. O., Rev. Sci. Instr. 25, 569 (1954).

2. Bastiansen, O., Hassell, O., and Risberg, E., Acta Chemica Scand. 9, 232 (1955).

3. DeNeui, R. J., An electron diffraction investigation of methane, deuteromethane and chlorine, unpublished M. S. thesis, Ames, Iowa, Library, Iowa State University of Science and Technology, 1961.

4. Dilthey, W., Zeit. fur angew. Chemie 34, 596 (1921).

5. Core, A. F., Chemistry and Industry 5, 642 (1927).

6. Nekrason, B. V., J. Gen. Chemistry (URSS) 10, 1021 (1940).

7. Bauer, S. H., J. Chem. Phys. 59, 1096 (1937).

8. Hipple, J. A., Jr., Physical Rev. 57, 350 (1940).

9. Mark, H. and Pohland, E., Zeit. fur Krist. 62, 103 (1925).

10. Stitt, F., J. Chem. Phys. 9, 780 (1940).

11. Longuet-Higgens, H. C. and Bell, R. P., J. Chem. Soc. 250 (1943).

12. Stitt, F. J., Chem. Phys. 9, 780 (1941).

13. Pitzer, K. S., J. Am. Chem. Soc. 67, 1126 (1945).

14. Mulliken, R. S., Chem. Rev. 41, 207 (1947).

15. Price, W. C., J. Chem. Phys. 15, 614 (1947).

16. Price, W. C., J. Chem. Phys. 16, 894 (1948).

17. Hedberg, K. and Schomaker, V., J. Chem. Phys. 16, 894 (1948).

18. Lipscomb, W. N., J. Chem. Phys. 22, 985 (1954).

19. Eberhardt, W. H., Crawford, B. and Lipscomb, W. N., J. Chem. Phys. 22, 989 (1954).

20. Pauling, L., Nature of the chemical bond, 3rd ed., Ithaca, New York, Cornell University Press, 1960.

21. Rundle, R. E., J. Am. Chem. Soc. 69, 1327 (1947).

22. Rundle, R. E., J. Chem. Phys. 17, 671 (1949).

23. Levy, H. A. and Brockway, L. O., J. Am. Chem. Soc. 59, 2085 (1937).

24. Bauer, S. H., J. Am. Chem. Soc. 59, 1804 (1937).

25. Bauer, S. H. and Beach, J. Y., J. Am. Chem. Soc. 63, 1394 (1941).

26. Bauer, S. H. and Hastings, J. J., J. Am. Chem. Soc. 64, 2686 (1942).

27. Sutton, L. E., Tables of interatomic distances and configuration in molecules and ions, London, The Chemical Society, 1958.

28. Pauling, L. and Brockway, L. O., J. Chem. Phys. 2, 870 (1934).

29. Elliott, A., Roy. Soc. London, Proc. A123, 638 (1930).

30. Richards, W. G. and Barrow, R. F., Chem. Soc. London, Proc. 297 (1962).

31. Degard, C., Pierard, J. and Van der Grinten, W., Nature 136, 142 (1935).

32. Bonham, R. A. and Bartell, L. S., J. Chem. Phys. 31, 702 (1959).

33. Bartell, L. S., Kuchitsu, K. and DeNeui, R. J., J. Chem. Phys. 35, 1211 (1961).

34. Hauptman, H. and Karle, J., Physical Rev. 77, 491 (1950).

35. Atoji, M., Acta Cryst. 10, 291 (1956).

36. Bewilogua, L., Physik. Zeitshrift 32, 740 (1931).

37. Degard, C., Soc. Roy. Sciences Liege, Bull. 12, 383 (1937).

38. Bartell, L. S., Brockway, L. O. and Schwendeman, R. H., J. Chem. Phys. 23, 1854 (1955).

39. Kutchitsu, K. and Bartell, L. S., J. Chem. Phys. 35, 1945 (1961).

40. Bonham, R. A. and Ukaji, T., J. Chem. Phys. 36, 72 (1962).

41. Bartell, L. S. and Brockway, L. O., J. Chem. Phys. 32, 512 (1960).

42. Bartell, L. S., J. Applied Phys. 31, 252 (1960).

43. Mark, H. and Wierl, R., Naturwissenschaften 18, 205 (1930).

44. Linnik, Yu. V., Method of least squares and principles of the theory of observations, New York 22, N. Y., Pergamon Press, Inc., 1961.

45. Whittaker, E. T. and Robinson, G., Calculus of observations, 4th ed., New York, D. Van Nostrand, 1952.

46. Bartell, L. S., J. Chem. Phys. 23, 1219 (1955).

47. Almenningen, A., Bastiansen, O. and Munthe-Kaas, T., Acta Chemica Scand. 10, 261 (1956).

48. Almenningen, A., Bastiansen, O. and Traetteberg, M., Acta Chemica Scand. 13, 1699 (1959).

49. Kohl, D., Ames, Iowa, Generalized program for the calculation of synthetic intramolecular distances, private communication, 1962.

50. Naylor, R. E., Jr. and Wilson, E. G., J. Chem. Phys. 26, 1057 (1957).

51. Scott, D. W., J. Am. Chem. Soc. 81, 1015 (1959).

52. Cruickshank, D. W., J. Acta Cryst. 2, 65 (1949).

53. Hedberg, K. and Stosick, A. J., J. Am. Chem. Soc. 74, 954 (1952).

54. Jones, M. E., Hedberg, K. and Schomaker, V., J. Am. Chem. Soc. 75, 4116 (1953).

55. Nordman, C. E. and Lipscomb, W. N., J. Chem. Phys. 21, 1856 (1953).

56. Hrostowski, H. J. and Myers, R. J., J. Chem. Phys. 22, 262 (1954).

57. Hirshfeld, F. L., Eriks, K., Dickerson, R. E., Lippert, E. L. and Lipscomb, W. N., J. Chem. Phys. 28, 56 (1958).

58. Kasper, J. S., Lucht, C. M. and Harker, D., Acta Cryst. 3, 436 (1950).

59. Lucht, C. M., J. Am. Chem. Soc. 73, 2373 (1951).

60. Gordy, W., Ring, H. and Burg, A. B., Physical Rev. 78, 512 (1950).

61. Atoji, M. and Lipscomb, W. M., J. Chem. Phys. 23, 217 (1955).

V. ACKNOWLEDGMENTS

I wish to thank Dr. L. S. Bartell for the assistance and advice given during the course of this research.

I would also like to express my gratitude to Dr. K. Kuchitsu for his help given in the use of the electron diffraction unit.

For the aid which has been freely given during the past four years I would like to thank Harlan Higginbotham and Jack Guillory.

I am also beholden to Dr. E. Roth for proof reading earlier drafts of the thesis.

And finally I wish to thank my wife for the patience and understanding she has shown during the course of this study.